Ab initio calculations of the $SrTiO_3$ (110) polar surface

E. Heifets* and W. A. Goddard III
Materials and Process Simulation Center, Beckman Institute, California Institute of Technology, MS 139-74, Pasadena, California 91125, USA

E. A. Kotomin
Institute for Solid State Physics, University of Latvia, 8 Kengaraga, Riga LV-1063, Latvia and Max Planck Institut für Festkörperforschung, Heisenbergstrasse 1, D-70569 Stuttgart, Germany

R. I. Eglitis and G. Borstel
Universität Osnabrück, Fachbereich Physik, D-49069 Osnabrück, Germany

(Received 8 May 2003; revised manuscript received 21 August 2003; published 21 January 2004)

Results of *ab initio* Hartree-Fock calculations for the $SrTiO_3$ (110) polar surface are discussed. We have calculated the surface energies, near-surface atomic displacements for four possible terminations (TiO, Sr, and two kinds of O terminations) as well as Mulliken atomic charges and dipole moments of atoms characterizing their polarization, and the atomic bond populations. We predict a considerable increase of the Ti—O chemical bond covalency near the (110) surface, as compared to both the bulk and the (100) surface. The O-terminated (110) surface has surface energy close to that for (100), which indicates that both (110) and (100) $SrTiO_3$ surfaces can coexist in polycrystals and perovskite ceramics.

DOI: 10.1103/PhysRevB.69.035408 PACS number(s): 68.35.Bs, 68.35.Md, 68.47.Gh

I. INTRODUCTION

Many technological applications, including catalysis, microelectronics, substrates for growth of high T_c superconductors, etc., are based on thin films of ABO_3 perovskite ferroelectrics.[1–4] Several *ab initio* quantum-mechanical[5–11] and classical shell model (SM) (Refs. 12-17) theoretical studies dealt with the (100) surface of $BaTiO_3$ and $SrTiO_3$ crystals (hereafter BTO and STO). Recently,[18] a reconstruction of the (relatively simple) (100) surface was studied experimentally and theoretically, which resulted in a novel model of TiO_2-rich surface.

In order to study dependence of the surface relaxation properties on exchange–correlation functionals and localized/plane-wave basis sets used in calculations, we performed recently a detailed comparative study of (100) $SrTiO_3$ surfaces based on ten different quantum-mechanical techniques.[19–21] The main conclusion drawn there was that the Hartree-Fock (HF), density-functional theory (DFT), and SM calculations give quite similar results for the (100) atomic structure relaxation and surface energies.

The STO (110) polar perovskite surface was studied experimentally using several different techniques. Low-energy electron diffraction (LEED) shows a number of surface reconstructions at high temperatures, atomic force microscopy also supports surface modification due to applied extensive thermal treatment.[22–24] However, there are no experimental estimates of the surface relaxation of the STO or BTO (110) surfaces at low temperatures, to which we could compare our calculations.

Only a few semiempirical quantum-mechanical calculations[4,25,26] exist so far for the (110) perovskite surfaces. The first *ab initio* study[27] was published when our paper was submitted recently for publication. In the paper[27] the local-density approximation method in the frame of DPT(DFT-LDA) with plane waves was used, which is quite different from our HF-localized basis set approach. As we demonstrate below, results of these two approaches agree quite well and complement each other.

We performed recently semiempirical SM calculations of the atomic relaxation for the polar (110) surfaces of STO and BTO.[17] In this paper, we discuss results of *ab initio* quantum-mechanical calculations of the relaxed atomic structure for four different terminations of the STO (110) surfaces.

II. METHODS AND SURFACE MODELS

We performed simulations of STO perovskite in the cubic crystalline phase, stable above 105 K. We use the CRYSTAL–98 computer code (see Ref. 28 and references therein for a description of all techniques mentioned here), in which HF and DFT types of calculations are both implemented. Unlike the plane–wave codes employed in most previous calculations, CRYSTAL–98 uses localized Gaussian-type basis sets. In our simulations we applied the basis set recommended for $SrTiO_3$ (Ref. 28). An additional advantage of the CRYSTAL–98 code is that it treats isolated two-dimensional (2D) slabs, without an artificial periodicity in the *z* direction perpendicular to the surface, as commonly employed in all previous surface–band structure calculations (e.g., Refs. 5,11). We restrict ourselves to the HF calculations, since this method gives for the (100) surface results quite similar to the DFT and hybrid methods.[20,21]

We calculate displacements of the atomic coordinates in several planes near the surface, where we calculate the effective atomic charges and bond populations between nearest atoms in order to characterize the effect of covalency, as well as the atomic dipole moments characterizing the atomic polarization and electronic density deformation near the surface. These options of the quantum chemical approach,

 ©2004 The American Physical Society

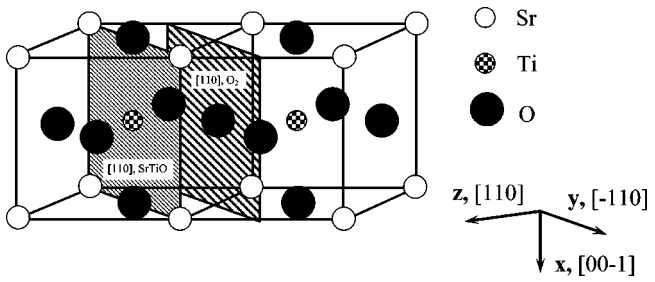

FIG. 1. Schematic view of the two (110) surface terminations: O—O and SrTiO. Arrows indicate the axis directions.

which are absent in the plane-wave calculations, permit us to learn about fine details of the electronic structure of surfaces of partly ionic solids like perovskites.

Note that the atomic effective charge is not uniquely defined. We use here the standard Mulliken population analysis.[28] Another option could include the dynamical Born charges,[29] the Bader charges[30] based on the topological analysis of the electron density, which corresponds to a partition of the total charge into atomic basins, etc. The atomic dipole moments are calculated in the CRYSTAL code as matrix elements of atomic orbitals with the operator z directed outward from the surface. This characterizes the shift of the atomic electron density along the axis normal to the surface. Our analysis of the electron-density redistribution is accompanied by the difference electron-density maps. These are calculated as the total HF electron density minus a superposition of the densities for isolated ions (O^{2-}, Ti^{4+}, and Sr^{2+}).

For optimization of atomic coordinates through minimization of the total energy per unit cell, we use our own computer code that implements the conjugated gradients optimization technique with numerical computation of energy derivatives (forces). Using this code, we optimized the atomic positions in three top layers of a STO slab consisting of seven planes, so that the top and bottom planes are the same (e.g., TiO).

Unlike the (100) neutral surface, the problem in modeling the (110) polar surface (Fig. 1) is that it consists of charged planes, O-O or SrTiO. If one assumes fixed ionic charges O^{2-}, Ti^{4+}, and Sr^{2+} (which is the case for SM calculations), then modeling of the (110) surface exactly as would be obtained from a perfect-crystal cleavage leads either to an infinite macroscopic dipole moment perpendicular to the surface, when the slab is terminated by planes of different kinds (O_2 and SrTiO), or to the infinite charge, when it is terminated by the same type of crystalline planes (O_2—O_2 or SrTiO—SrTiO). It is known that such crystal terminations make the surface unstable.[4,31] In real quantum-mechanical calculations for a finite-thickness slab terminated by the different kind of planes the charge redistribution near the surface arising during the self-consistent-field (SCF) procedure, could, in principle, compensate the macroscopic dipole moment. On the other hand, in the calculations of slabs terminated by similar planes the charge neutrality could be easily retained by setting in the computer inputs an appropriate number of electrons or just zero net charge of the unit cell. However, careful studies[4,25,27] demonstrate that these two options for STO surfaces are energetically expensive with respect to the dipole moment elimination via introduction of vacancies.

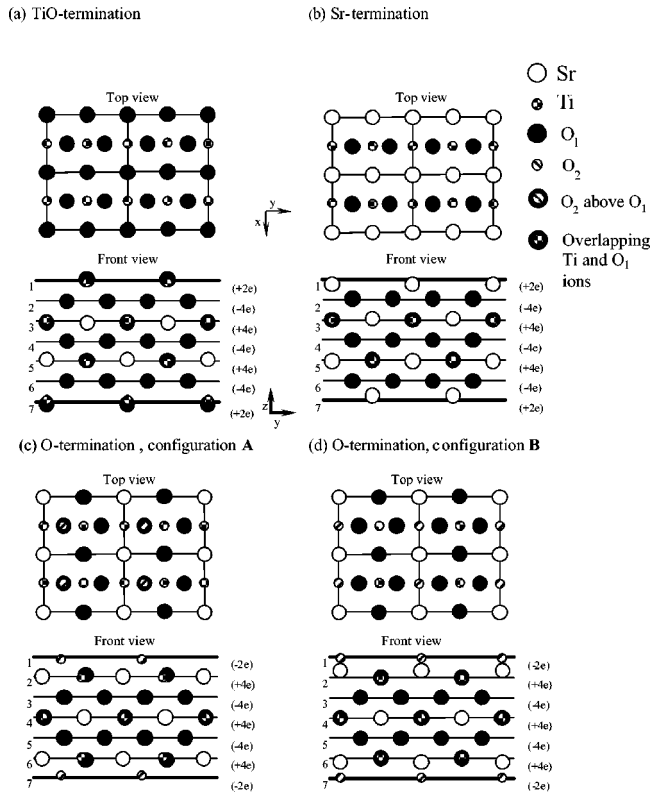

FIG. 2. The top and front view of four possible terminations for the (110) perovskite surfaces. For the asymmetric and symmetric O terminations, (c) and (d), respectively, the top plane contains only atoms O_2 whereas atoms O_1 lie in the second SrTiO plane, see Fig. 1 and details in the text. Note that some O_1 atoms overlap with O_2 and Ti atoms as indicated in the legend.

This is why in our calculations we removed half the O atoms from the O-terminated surface, and Sr or both Ti and O atoms from the SrTiO- terminated surface [called hereafter for the simplicity O-, TiO-, and Sr- terminated surfaces, see Figs. 2(a)–2(d)]. As a result, our surface with charged planes has a zero dipole moment (before atomic relaxation).

The initial atomic configuration for the O-terminated surface, where every second surface O atom is removed and others occupy the same sites as in the bulk structure, is called *asymmetric* (*A*) configuration hereafter [see O_2 ions in Fig. 2(c)]. Since such a removal of half the O atoms seems to disturb the balance of interatomic forces along the surface, we also studied another *symmetric* initial surface configuration (*B*) in which the O_2 atom is placed in the *middle* of the distance between two equivalent O atoms in the bulk [Fig. 2(d)]. Computations of the *A*-type surface reveal considerable atomic displacements not only perpendicular to the surface, but also parallel to the surface. Preliminary SM results for the *A* and *B* cases were discussed in Ref. 17.

In order to calculate the surface energy for the TiO- and Sr terminated surfaces, we start with the *cleavage energy* for unrelaxed surfaces. In our calculations the two seven-plane Sr- and TiO-terminated slabs represent together seven bulk

unit cells. The surfaces with both terminations arise simultaneously under cleavage of the crystal and the relevant cleavage energy is divided equally between these two surfaces. Therefore, we assume that the cleavage energy is the same for both terminations

$$E_s^{(unrel)} = \tfrac{1}{4}[E_{slab}^{(unrel)}(\mathrm{Sr}) + E_{slab}^{(unrel)}(\mathrm{TiO}) - 7E_{bulk}], \quad (1)$$

where $E_{slab}^{(unrel)}(\mathrm{Sr})$ and $E_{slab}^{(unrel)}(\mathrm{TiO})$ are energies of the unrelaxed slabs, E_{bulk} is the energy per bulk unit cell, and 1/4 means that totally four surfaces were created upon the crystal cleavage. Next we calculate the (negative) relaxation energies for each of the Sr- and TiO terminated surfaces, when both sides of slabs are allowed to relax

$$E_{rel}(A) = \tfrac{1}{2}[E_{slab}(A) - E_{slab}^{(unrel)}(A)], \quad (2)$$

where $E_{slab}(A)$ is the slab energy after the relaxation, A = Sr or TiO. Finally, the surface energy sought for is just a sum of the cleavage and relaxation energies

$$E_s(A) = E_s^{(unrel)} + E_{rel}(A). \quad (3)$$

When we cleave the STO crystal in another way, we obtain two identical O-terminated surfaces. This allows to simplify the calculations. Note that the unit cell of the seven-plane O-terminated slab contains three bulk unit cells. Therefore, the relevant surface energy is

$$E_s(\mathrm{O},\alpha) = \tfrac{1}{2}[E_{slab}(\mathrm{O},\alpha) - 3E_{bulk}], \quad (4)$$

where $E_s(\mathrm{O},\alpha)$ and $E_{slab}(\mathrm{O},\alpha)$ are the surface energy and the slab total energy for the O-terminated surface in the symmetric and asymmetric configurations A and B described above ($\alpha = A,B$, respectively).

The Mulliken effective charges for Ti and O ions, both in the bulk ($2.59e$ and $-1.50e$, respectively) and on the (100) surface calculated from the HF and DFT wave functions[20] are much smaller, than formal ionic charges ($4e$ and $-2e$, respectively). This arises due to the partly covalent nature of the Ti—O chemical bond. In contrast, the Sr charge remains close to the formal charge, $+2e$. The covalency of the Ti—O chemical bond is confirmed by calculated bond populations, which vary from $0.05e$ (DFT–LDA) to $0.11e$ (HF), depending on the particular method. Obviously, there is no chemical bonding between any other types of atoms, e.g., Sr—O or O—O. For comparison, the following Bader atomic charges were calculated for the O, Ti and Sr ions in the STO bulk:[27] $-1.26e$, $2.18e$, and $1.58e$, respectively. The first two charges are slightly smaller than our Mulliken charges but the Sr charge is obviously too small since there is no indication for the chemical bonding between Sr and O in STO.[20,21]

The atomic displacements in the (100) outermost $SrTiO_3$ planes, obtained by means of various *ab initio* methods, were analyzed in Refs. 20, 21. We stress here only that our Gaussian-basis results are in good agreement with previous plane-wave calculations.[5,11] Both DFT and HF calculations predict larger Sr displacement on the SrO-terminated surface, than that for Ti atom on the TiO_2-terminated surface, in agreement with previous *ab initio* plane-wave calculations. For the TiO_2 termination, *all* theoretical methods predict that the surface O atom relaxes inwards, in contrast to the SrO termination. Relaxation of atoms in the third plane was found to be quite small, indicating that relaxation of three layers is adequate.

Calculations of the (100) surfaces show that the surface energy of the SrO-terminated surface is only slightly smaller, than the surface energy of TiO_2-terminated surface. Thus, both types of (100) surfaces can coexist, in agreement with the experimental observation.[20]

III. MAIN RESULTS

A. Surface energies and atomic relaxation

Table I demonstrates good agreement for the *surface energies*, calculated using the HF and the SM (in both cases results correspond to three relaxed planes). Unlike the (100) surface, we see that different terminations of the (110) surface lead to great differences in the surface energies. Here the lowest energy has the *A*-type O-terminated surface. The surface energy per unit cell for the *A*-type O-terminated surface (1.40 eV) is approximately the same as for the (100) surfaces (1.38–1.42 eV from HF calculations[20]). The DFT-LDA calculations[27] for the O termination give the surface energy of 1.2 eV, close to our results.

The HF–calculated atomic relaxations for STO (110) surface, shown in Table II, confirm results of much simpler SM calculations. The agreement between HF and SM for all four termination is remarkable indeed. This demonstrates that semiempirical classical calculations with a proper parametrization can serve as a very useful tool for modeling perovskite thin films. An idea about the nature of the relaxed (110) surfaces can be obtained from Fig. 2 (see front views). On the TiO-terminated surface, Ti atoms move inward (towards the bulk), whereas O atoms move outward (towards the vacuum), by a similar distance ($0.06a_0$–$0.07a_0$). Sr atoms in the top layer of the Sr-terminated surface move inward much more, by $0.17a_0$. The O ions in the top layer of the *A*-type O-terminated surface also move inward, more than by $0.10a_0$, in the direction almost perpendicular to the O(I)—Ti(II) bond. Ti atoms on this surface move along the surface, by $0.08a_0$, and also slightly inward. Sr atoms move almost in the same *y* direction, by a similar distance, but also slightly, $0.02a_0$, outward the slab. The second-layer O ions move by $0.06a_0$ in the direction opposite to that for the top-layer O ions, whereas the third-layer O ions displace more than that but inward, that is, in the same direction as the top-layer O ions. The atomic displacements were also optimized in the DFT-LDA calculations[27] for the O-terminated surface assuming no on-plane relaxation. The results for the *z* displacements are qualitatively similar to ours: the top O atoms strongly go inward, as well as Ti atoms in the second plane, whereas the Sr and O atoms in the second plane move outward.

Ions on the *B*-type O-terminated surface move only perpendicularly to the surface, as expected by the symmetry. The O atoms in the top layer and Ti atoms in the second layer, both move by $0.4a_0$ inward, whereas the second-layer

TABLE I. Surface energies (in electronvolt per unit cell area) for the four different O (110) terminations shown in Fig. 2, as calculated using HF and SM.[17] In both cases three near-surface planes were relaxed.

Type	HF	SM
O terminated, *A* type	1.40	1.54
B type	3.08	3.13
TiO	2.10	2.21
Sr	2.97	3.04

O atoms move outward, by $0.08a_0$. The Sr atoms from the same second layer move outward, by a very large distance of $0.23a_0$. This relaxation was predicted earlier in our SM calculations[17] (see Table II). Atomic displacements in the third plane from the surface are still large. This is in sharp contrast with previous results[20,21] for the neutral (100) surfaces, where atomic displacements converge very fast and are already very small in the third layer.

B. Electronic charge distribution

We calculated the Mulliken effective charges Q, their changes ΔQ, with respect to the bulk values, and dipole moments d for atoms near the surface (Table III). In addition, we analyzed the charge redistribution between different layers in slabs with all terminations (Table IV). The charge of the surface Ti atoms in the TiO terminated is reduced by $0.15e$. Metal atoms in the third layer lose much less charge. O ions in all layers, except the central one, also reduce their charges, making them less negative. The largest charge change is observed for subsurface O atoms $(0.28e)$. This gives a large positive change of $0.56e$ in the charge for each subsurface layer. Consequently, the additional net charge of $0.84e$ $(0.42e$ per surface), calculated for the TiO-terminated slab with respect to the bulk charges, is concentrated in the subsurface layers. The negative charge density changes in other layers of this slab reduce the additional surface charge density of the TiO-terminated surface.

On the Sr-terminated surface, negative changes in the charge are observed for all atoms except for oxygen in the central layer. The largest changes are at the surface Sr ion $(-0.13e)$ and at the Ti ion in the third layer $(-0.16e)$. The largest change in the charge density $(-0.22e)$ appears in the third layer as well. In the present 7-layer slab model an additional negative charge density of $-0.82e$ $(-0.41e$ per surface) accumulated in the Sr-terminated slab with respect to the bulk charges, is spread over three top layers on each side of the slab. Two types of surface structures for O-terminated slabs, which we denote as *A* and *B*, show very different charge redistributions. For the *A*-type structure, the negative charge on the surface oxygen is decreased $(\Delta Q=0.20e)$, but for the *B*-type structure, it increases $(\Delta Q=-0.16e)$.

In both structures the charge change in the second layer is negative. In the *A*-type structure this change $(-0.10e)$ comes mostly from O atom $(-0.09e)$. In the *B*-type structure, the change $(-0.14e)$ appears mostly due to a decrease of Sr atom charge $(-0.17e)$. The charge density of the third layer in the *A*-type slab is almost unchanged. In the *A*-type structure two different oxygens in the third layer are nonequivalent. Their charge change is almost equal, but in the opposite directions. In contrast, for the *B*-type structure these oxygens are equivalent by symmetry, and their charges change less $(0.12e)$. This leads to a positive change $(0.24e)$ of the charge density in the third layer. Charge densities of the central layer for the *A* and *B* structures change again in the opposite directions.

We note here that when the STO crystal is cleaved along the (110) surface, the TiO- and Sr-terminated surfaces are formed simultaneously. These surfaces complement each other to the crystalline bulk. Therefore, the total slab charges of these two surfaces with respect to the bulk charges should be equal in magnitude but with opposite signs. Indeed we obtain just this result in the present simulations (Table IV). Similarly, crystal cleavage can produce two identical surfaces with one O atom per surface unit cell. The total charge of such O-terminated surfaces should be zero, due to its stoichiometry.

Atomic polarization is large in all layers of all slabs, except for the central plane. (This happens because the electric fields in this layer caused by other planes are canceled by the symmetry.) Indeed, we find that the dipole moments of many Sr ions are comparable, and sometimes significantly larger

TABLE II. Atomic relaxation of three top layers (in percent of the lattice constant) for four terminations, calculated by means of the *ab initio* HF and shell model (Ref. 17). Positive sign corresponds to outward atomic displacements (toward the vacuum).

Layer	Atom	SM δz	SM $\overline{\delta y}$	HF δz	HF $\overline{\delta y}$
Ti—O terminated					
1	Ti	−5.99		−6.49	
1	O	8.48		6.85	
2	O	−1.72		−1.47	
3	O	−4.10		−3.85	
3	Ti	2.14		2.20	
3	Sr	−6.96		−5.78	
Sr terminated					
1	Sr	−19.07		−17.38	
2	O	3.18		2.72	
3	Sr	4.67		3.95	
3	O	−0.25		−0.21	
3	Ti	−0.89		−0.86	
O terminated	*A* type				
1	O	−14.2	−8.54	−10.41	−10.53
2	Ti	−2.37	−8.27	−1.36	−7.71
2	Sr	4.10	−10.79	2.20	−7.30
2	O	5.71	8.20	6.65	6.15
3	O	−11.06	−11.01	−7.02	−7.46
O terminated	*B* type				
1	O	−2.78		−3.95	
2	Ti	−5.14		−4.26	
2	Sr	30.32		22.67	
2	O	9.68		8.23	
3	O	−2.41		−1.68	

TABLE III. Calculated Mulliken atomic charges Q (in e) changes in atomic charges ΔQ with respect to the bulk charges (in e), and dipole moments of atoms, d (in e a.u.) for four terminations. The Mulliken charges in the bulk are: $2.59e$ (Ti), $-1.50e$ (O), and $1.91e$ (Sr).

Atom (layer)	Q	ΔQ	d
Ti—O terminated			
Ti(I)	2.44	−0.15	−0.23
O(I)	−1.39	0.10	0.05
O(II)	−1.22	0.28	0.07
Sr(III)	1.88	−0.03	0.22
Ti(III)	2.56	−0.02	0.11
O(III)	−1.48	0.02	0.10
O(IV)	−1.56	−0.06	0.00
Sr termination			
Sr(I)	1.78	−0.13	0.38
O(II)	−1.55	−0.05	0.09
Sr(III)	1.90	−0.01	−0.00
Ti(III)	2.43	−0.16	0.21
O(III)	−1.55	−0.05	−0.14
O(IV)	−1.46	0.04	0.00
O termination	*A* type		
O(I)	−1.30	0.20	0.21
Sr(II)	1.89	−0.02	0.02
Ti(II)	2.59	0.01	0.07
O(II)	−1.59	−0.09	0.08
O(III)	−1.33	0.17	0.06
O(III)	−1.66	−0.16	0.69
Sr(IV)	1.92	0.01	0.00
Ti(IV)	2.43	−0.15	0.00
O(IV)	−1.58	−0.08	0.00
O termination	*B* type		
O(I)	−1.66	−0.16	0.23
Sr(II)	1.74	−0.17	−0.19
Ti(II)	2.62	0.04	−0.19
O(II)	−1.51	−0.01	0.04
O(III)	−1.38	0.12	0.10
Sr(IV)	1.90	−0.01	0.00
Ti(IV)	2.67	0.09	0.00
O(IV)	−1.45	0.05	0.00

than the dipole moments of O ions. This indicates their strong polarization. We observed earlier the same result for the (100) surfaces.[20,21] The dipole moment of the surface Ti ions on the TiO-terminated surface are directed inward (toward the bulk). This is the only case among the surfaces that we considered, in which the ions in the top-layer polarized in this way. The dipole moments of the oxygen atoms in the first two layers on this surface are directed outward the surface, being a factor of 3–4 less than those of the surface Ti. In the third layer, the dipole moment of Sr ions has a value similar to that for the surface Ti but directed outward. The dipole moments of other ions in this layer are about a half of the dipole moment of the Sr.

On the Sr-terminated surface, the dipole moment of the surface Sr atoms are directed outward and are large ($0.38e$ a.u.). Polarization of the O atoms in the next layer is by a factor of 4 smaller. Polarizations of the Ti and O ions in the third layer are larger and opposite in their directions: outward for the surface Ti ($0.21e$ a.u.) and inward for O ions ($0.14e$ a.u.). At both O-terminated surfaces, oxygens are polarized outward. On the *A*-type surface the atomic polarization in the second layer is directed outward and much smaller than that for the surface O ions. On the *B*-type surface, dipole moments of the metal atoms in the second layer are directed inward, but about 20% smaller than the dipole moment of the surface O.

TABLE IV. Charge density (per unit cell) and its change (with respect to the bulk), as calculated for four top planes and four different terminations of the (110) surface. The charges of planes 5–7 are the same by symmetry as for planes 1–3.

Unit (layer)	Q	ΔQ
Ti—O terminated		
TiO(I)	1.04	−0.05
O_2(II)	−2.44	0.56
SrTiO(III)	2.97	−0.03
O_2(IV)	−3.12	−0.12
Sr termination		
Sr(I)	1.78	−0.13
O_2(II)	−3.10	−0.10
SrTiO(III)	2.78	−0.22
O_2(IV)	−2.92	0.08
O termination	*A* type	
O(I)	−1.30	0.20
SrTiO(II)	2.89	−0.10
O_2(III)	−2.99	0.01
SrTiO(IV)	2.77	−0.22
O termination	*B* type	
O(I)	−1.66	−0.16
SrTiO(II)	2.85	−0.14
O_2(III)	−2.76	0.24
SrTiO(IV)	3.12	0.13

C. Chemical bonding

The interatomic *bond populations* for four possible terminations are given in Table V. The major effect observed here is a strong increase of the Ti—O chemical bonding near the surface as compared to (already large) bonding in the bulk (112 me). For the O-terminated *A*-type surface the O(I)–Ti(II) bond population is as large as 294 me, i.e., by a factor of two larger than that in the bulk. [This factor for the (100) surface[21] was 1.5.] The Ti—O bond population reaches practically the bulk value for atoms in a third plane. The increased Ti—O bond population near the (110) surface does not arise from surface relaxation. Our calculations demonstrate that for the TiO-terminated surface, the bond population for unrelaxed surface P[Ti(I)—O(II)] = 182 me increases up to 240 me after the surface relaxation. Second, for the same interatomic distance on the unrelaxed surface, the

TABLE V. The A—B bond populations, P (in milli $e=me$) and the relevant interatomic distances R (in Å) for three different O (110) terminations in STO. Symbols I–IV denote the number of each plane enumerated from the surface. The nearest neighbor Ti—O distance in the unrelaxed lattice is 1.945 Å.

Atom A	Atom B	P	R
Ti—O terminated			
Ti(I)	O(I)	176	2.01
	O(II)	240	1.81
O(II)	Ti(III)	140	1.85
	Sr(III)	−10	2.84
	O(III)	−22	2.80
Ti(III)	Sr(III)	0	3.38
	O(III)	126	1.96
	O(IV)	108	2.00
Sr(III)	O(III)	−22	2.75
	O(IV)	−24	2.64
O(III)	O(IV)	−24	2.68
Sr terminated			
Sr(I)	O(II)	−30	2.46
O(II)	Sr(III)	−26	2.73
	Ti(III)	208	2.05
	O(III)	−8	2.81
Sr(III)	O(III)	−22	2.76
	O(IV)	−14	2.83
Ti(III)	O(III)	116	1.95
	Sr(III)	0	3.37
	O(IV)	112	1.92
O(III)	O(IV)	−30	2.75
O terminated	A type		
O(I)	Sr(II)	−28	2.47
	Ti(II)	294	1.80
	O(II)	−26	2.90
Sr(II)	O(II)	−30	2.23
	Ti(II)	0	3.36
Ti(II)	O(II)	90	2.04
	O(III)	104	2.10
O(II)	O(III)	−28	2.85
Sr(II)	O(III)	−6	2.94
O(III)	O(IV)	−20	2.48
	Ti(IV)	110	2.00
	Sr(IV)	−14	2.48
O terminated	B type		
O(I)	Sr(II)	−30	1.97
	Ti(II)	16	3.08
	O(II)	−4	3.49
Sr(II)	O(II)	−20	2.81
	Ti(II)	0	3.53
Ti(II)	O(II)	130	2.00
	O(III)	204	1.87
O(II)	O(III)	−18	2.96
Sr(II)	O(III)	4	3.33
O(III)	O(IV)	−22	2.72
	Ti(IV)	114	1.90
	Sr(IV)	−22	2.72

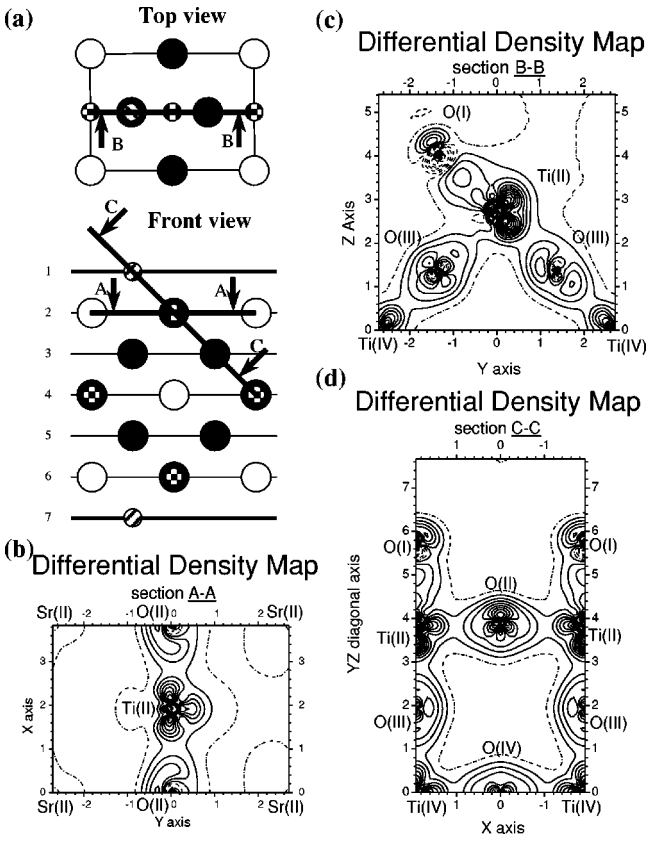

FIG. 3. Three cross sections (a) and the relevant difference electron density maps (b)–(d) for the O-terminated asymmetric (A-type) (110) surface. Densities are calculated with respect to the superpositions of the Ti^{4+}, O^{2-}, and Sr^{2+} ion densities. Full and dashed lines correspond to the excess and deficiency of the electron density. The increment is 0.01 e/a.u.^{3}.

Ti—O bond populations are larger in the direction *perpendicular* to the surface (182 me) than in-plane (126 me).

There are no O atoms on the Sr-terminated surface. However, the bond population between O(II) and Ti(III) atoms is 208 me, larger than in the bulk (and also larger than on-plane, O(III)—Ti(III) bond population). Finally, for the B-type surface, the O(I)—Ti(II) bond population is small, due to a large distance between the two atoms in this specific configuration. (Probably, this is the reason why B termination has such a large surface energy.) However, the Ti(II)—O(III) bond population is again large and close to that for O(II)—Ti(III) on the Sr-terminated surface.

These effects are obvious on the *difference electron-density maps* for the unrelaxed O-terminated A-type surface shown in Fig. 3. The cross-section AA shows clearly the Ti(II)—O(II) in-plane bonding in the second plane ($P=90$ me). (On the TiO terminated surface $P=126$ me.) Cross section BB demonstrates asymmetry in the Ti—O bonding between the Ti and O atoms in the first, second, and third planes. The electron density on O atoms in third plane is considerably more localized than that in the first plane. Finally, the diagonal cross-section CC confirms our conclusions that the strongest covalent bonding is formed between

O(I) and Ti(II), whereas the covalent bonding for Ti(II)—O(II) and Ti(II)—O(III) are similar.

IV. CONCLUSIONS

Summing up, our *ab initio* calculations indicate a considerable increase of the Ti—O bond covalency near the (110) surface relative to bulk STO, much larger than that for the (100) surface. This should have an impact on the electronic structure of surface defects (e.g., *F* centers), and should affect the adsorption and surface diffusion of atoms and small molecules relevant for catalysis. The atomic displacements calculated by means of classical SM are surprisingly in good agreement with the *ab initio* HF calculations for STO. We find the O-terminated *A*-type surface has the lowest surface energy amongst all (110) terminations studied. This energy is close to that obtained for the (100) surface, i.e., both (100) and (110) STO surfaces can coexist in STO ceramics. The same conclusion was drawn in quite different DFT-LDA plane-wave calculations.[27] This means that the cancellation of a macroscopic polarization of polar surfaces by a formation of O vacancies thereon is much more efficient than a strong electronic-density redistribution and the relevant anomalous filling of the surface states which turns out to be energetically expensive.

We would like to note in conclusion that recently[32] we studied another O termination *C*, which corresponds to the 2×1 surface reconstruction, where O atoms are removed in pairs of nearest surface cells in a ''zig–zag'' way. We found that this has the surface energy only slightly lower than the configuration *A*.

ACKNOWLEDGMENTS

This study was partly supported by DFG (G. Borstel and R. Eglitis) and European Center of Excellence in Advanced Material Research and Technology in Riga, Latvia (Contract No. ICA–I–CT–2000–7007 to EK). In addition, partial support to E.H. and W.A.G. was provided by Grant No. DOE-FC26-02NT41631. Authors are greatly indebted to C.R.A. Catlow, S. Dorfman, R.A. Evarestov, J. Maier, and A.M. Stoneham for stimulating discussions.

*Corresponding author. Email address: heifets@wag.caltech.edu

[1] J. F. Scott, *Ferroelectric Memories* (Springer, Berlin, 2000).
[2] M. E. Lines and A. M. Glass, *Principles and Applications of Ferroelectrics and Related Materials* (Clarendon, Oxford, 1977).
[3] C. Noguera, *Physics and Chemistry at Oxide Surfaces* (Cambridge University Press, New York, 1996).
[4] C. Noguera, J. Phys.: Condens. Matter **12**, R367 (2000).
[5] J. Padilla and D. Vanderbilt, Surf. Sci. **418**, 64 (1998).
[6] J. Padilla and D. Vanderbilt, Phys. Rev. B **56**, 1625 (1997).
[7] B. Meyer, J. Padilla, and D. Vanderbilt, Faraday Discuss. **114**, 395 (1999).
[8] F. Cora and C.R.A. Catlow, Faraday Discuss. **114**, 421 (1999).
[9] R.E. Cohen, Ferroelectrics **194**, 323 (1997).
[10] L. Fu, E. Yaschenko, L. Resca, and R. Resta, Phys. Rev. B **60**, 2697 (1999).
[11] C. Cheng, K. Kunc, and M.H. Lee, Phys. Rev. B **62**, 10409 (2000).
[12] E. Heifets, S. Dorfman, D. Fuks, and E. Kotomin, Thin Solid Films **296**, 76 (1997).
[13] E. Heifets, S. Dorfman, D. Fuks, E. Kotomin, and A. Gordon, J. Phys.: Condens. Matter **10**, L347 (1998).
[14] D. Fuks, S. Dorfman, E. Heifets, A. Kotomin, and A. Gordon, in ''Structure and Evolution of Surfaces,'' edited by R. C. Cammarata, E. H. Chason, T. L. Einstein, and E. D. Williams, MRS Symposia Proceedings No. **440** (Materials Research Society, Pittsburgh, USA, 1997), p. 305.
[15] S. Dorfman, E. Heifets, D. Fuks, E. Kotomin, and J. Felsteiner, in ''Materials for Smart Systems II,'' edited by E. P. George, R. Gotthardt, and K. Otsuka, MRS Symposia Proceedings No. **459** (Materials Research Society, Pittsburgh, USA, 1997), p. 219.
[16] S. Tinte and M.G. Stachiotti, in *Fundamental Physics of Ferroelectrics 2000*, edited by Ronald E. Cohen, AIP Conf. Proc. No. 535 (AIP, Melville, NY, 2000).
[17] E. Heifets, E.A. Kotomin, and J. Maier, Surf. Sci. **462**, 19 (2000).
[18] N. Erdman, K. Poeppelmeler, M. Asta, O. Warschakow, and D.E. Ellis, Nature (London) **419**, 55 (2002).
[19] E.A. Kotomin, R.I. Eglitis, J. Maier, and E. Heifets, Thin Solid Films **400**, 76 (2001).
[20] E. Heifets, R.I. Eglitis, E.A. Kotomin, J. Maier, and G. Borstel, Phys. Rev. B **64**, 235417 (2001).
[21] E. Heifets, R.I. Eglitis, E.A. Kotomin, J. Maier, and G. Borstel, Surf. Sci. **513**, 211 (2002).
[22] K. Szot and W. Speier, Phys. Rev. B **60**, 5909 (1999).
[23] H. Bando, Y. Ochiai, Y. Aiura, Y. Haruyama, T. Yasue, and Y. Nishihara, J. Vac. Sci. Technol. A **19**, 1938 (2001).
[24] J. Brunen and J. Zegenhagen, Surf. Sci. **389**, 349 (1997).
[25] A. Pojani, F. Finocchi, and C. Noguerra, Surf. Sci. **442**, 179 (1999).
[26] A. Stashans and S. Serrano, Surf. Sci. **497**, 285 (2002).
[27] F. Bottin, F. Finocchi, and C. Noguera, Phys. Rev. B **68**, 035418 (2003).
[28] V. R. Saunders, R. Dovesi, C. Roetti, M. Causa, N. M. Harrison, R. Orlando, and C. M. Zicovich-Wilson, CRYSTAL-98 User Manual (University of Torino, Italy, 1999).
[29] R. Resta, Modell. Simul. Mater. Sci. Eng. **11**, R69 (2003).
[30] R. Bader, Chem. Rev. (Washington, D.C.) **91**, 893 (1991).
[31] P.W. Tasker, J. Phys. C **12**, 4977 (1979).
[32] E. Heifets, E. A. Kotomin, S. Dorfman, J. Maier, and W. A. Goddard III, Surf. Sci. (to be published).